X-RAY PHOTOELECTRON STUDY OF ELECTRON AND SPATIAL STRUCTURE OF MONO- AND BINUCLEAR Ni(II) CARBOXYLATE COMPLREXES WITH NITRIGEN-CONTAINING LIGANDS

A.G.Kochur[a], T.M.Ivanova[в], S. Hinder[c], J. Watts[c], A.A.Sidorov[в], M.A.Kiskin[в], V.M.Novotortsev[в], I.L.Eremenko[в]

[a] *Rostov State University of Transport Communication, Rostov-na-Donu, Russia*
[в] *Kurnakov Institute of General and Inorganic Chemistry of RAS, Moscow, Russia,*
[c]*The Surface Analysis Laboratory, School of Engineering (H6), University of Surrey, Guildford, UK*

Abstract

Ni3s, Ni3p and Ni2p x-ray photoelectron spectra of mono-and binuclear carboxylate complexes of nickel with various geometry of metal ions environment are obtained. The spectra are calculated in an isolated ion approximation. The dependence of the spectral profiles and the structure of the charge-transfer satellites on the structure of the immediate environment of nickel atoms is established. The data obtained support the results of X-ray diffraction and magnetic studies.

Introduction

Mono- and polynuclear carboxylate complexes of transition metals have diverse structures and a broad spectrum of chemical and physical (primarily magnetic) characteristics [1]. Carboxylate complexes of transition metals are promising in terms of their use in catalysis, enzymology, and also in preparation of medical products [2]. Many polynuclear transition metal complexes are molecular magnets [3, 4], in which transition metal atoms with unpaired 3d-electrons, isolated from the neighboring molecules by the shell of the ligands, form stable intramolecular ferro-antiferro- or ferrimagnetic structures [5].

X-ray photoelectron spectroscopy (XPS) has been successfully used to study the physical properties of metalloorganic complex. Various characterristics of X-ray photoelectron spectra of the transition metal complexes are sensitive to the electron density on the metal ion, on its spin state, and on geometry of the nearest environment of the met\al ion. This makes XPS an effective tool for the study of electronic, magnetic and spatial structure of the transition metal complexes.

In recent years, an increasing number of works devoted to the XPS studies of polynuclear transition metal complexes is seen. Polynuclear manganese complexes are studied in [6, 7]. Trimethylacetate polynuclear iron complexes are investigagted in [4, 8]. Cobalt complexes are studied in [9, 10].

The aim of this work is the XPS study of electronic structure of carboxylate nickel complexes with mono- and bidentate-coordinated amines of various types.

Peculiarity of nickel carboxylate complexes studied in this work is substantial variation in the geometry of the nearest environment of nickel ions when going from one compound to another; this must manifest itself in the photoelectron spectra.

Nickel complexes investigated in this work were previously studied by Ni2p-, Ni3p-, and N1s-spectra in [11], where the spectra were obtained at room temperature. In this paper, in order to eliminate possible influence of samples decomposition, Ni3s, Ni3p and Ni2p-spectra of the complexes were taken at liquid nitrogen temperature.

Assignment of the spectra is performed based on an isolated-ion approximation. The results of the previous calculations performed in refs [4, 6, 10] showed that this approximation, albeit rather crude, allows, however, to describe the basic details of the structure of the spectra and their change upon going from one compound to another.

Experimental

Photoelectron spectra of the compounds were taken with the spectrometer Thermo VG Scientific Sigma Prober (East Grinstead, UK). Characteristic Al$K\alpha_{12}$ radiation with the energy of 1486.6 eV was used for the excitation. All measurements were performed not less than twice at the pressure of ~10^{-9} torr. The spectra are taken at liquid nitrogen temperature. Calibration of the spectra was performed using the C1s-line assuming the binding energy (BE) of the C-(C, H) bond component to be 285.0 eV. In order to implement the calibration the decomposition of the spectra into components was performed in accordance with the structural formulas obtained with the X-ray diffraction analysis. Basic energies of functional groups present in the samples were taken from [12].

Theory

Relative energy positions of the initial- and final-state multiplets are calculated for the photoabsorption processes from 3s, 3p, and 2p subshells:

$$\mathrm{Ni}3s^2 3d^8 4s^2(^3F_4) + h\nu \rightarrow \mathrm{Ni}3s^1 3d^8 4s^2(^{2S+1}L_J) + \varepsilon p \quad (1)$$

$$\mathrm{Ni}3p^6 3d^8 4s^2(^3F_4) + h\nu \rightarrow \mathrm{Ni}3p^5 3d^8 4s^2(^{2S+1}L_J) + \varepsilon\{s,d\} \quad (2)$$

$$\mathrm{Ni}2p^6 3d^8 4s^2(^3F_4) + h\nu \rightarrow \mathrm{Ni}2p^5 3d^8 4s^2(^{2S+1}L_J) + \varepsilon\{s,d\} \quad (3)$$

where εl denotes a photoelectron with the kinetic energy ε.

In ionic configurations used in the calculations of the processes (1-3) 4s-electrons are used to simulate the electron density of the ligands in complexes of divalent nickel since the average radius of the Ni4s-shell (1.6 Å) is close enough to the metal-ligand distances.

Calculation of the multiplet structures and the photoionization cross sections (1-3) is performed in the intermediate coupling approximation by the methods described in [13] using the wave functions obtained in the Pauli-Fock approximation [14]. Natural level widths of the photoionization final states are calculated in the configuration-average approximation.

The principal effects determining the structure of 3*s*-, 3*p*-, and 2*p*-XPS of the transition metal atoms in compounds are:

- multiplet splitting in the final state of photoabsorption due to the electrostatic interaction of an inner-shell vacancy and unpaired electrons of the 3d-subshell;
- crystal field effects leading to the splitting of the 3d-subshell;
- screening of an inner-shell vacancy by ligands electrons giving rise to the charge-transfer satellites.

These effects are discussed in detail in numerous reviews and monographs, i.e. [15]. Most important among them is the multiplet splitting, which gives the grounds for using the isolated-ion approximation to calculate the structure of the XPS spectra of the compounds.

XPS spectra are additionally affected by a number of many-electron effects, chief among which is the reduction of atomic multiplets extentions due to the interaction of the states of the basic configuration with a lot of higher-lying excited configurations. As a rule, the structure of multiplets is not violated, and the compression of multiplets can be easily accounted for by scaling the integrals of electrostatic interaction, see, for example, [16]. Typically, the scaling factors are in the range of 0.7 to 0.8 [17] and they are selected on the basis of the best fit of calculated and experimental multiplets extentions.

In the case of the 3s-spectra, the effect of dipole polarization of electron shells (DPEO) is often large (see [18] and references therein). This effect is in strong interaction of 3s-photoionization final states $3s^1 3p^6 3d^N$ with energetically close states $3s^2 3p^4 3d^{N+1}$. As a result, a significant additional compression of the multiplet and distortion of its high-energy part take place, and correlation satellites appear at higher binding energies. An evidence of a significant effect of the DPEO is the need to introduce an abnormally small scaling factors for the exchange interaction integrals $G^2(3s,3d)$. For example, when calculating the 3s-spectra of manganese and iron in [4] and [6], the scaling factors obtained by fitting the calculated spectra to the experiment were found to be 0.45 and 0.43, respectively.

Basics of the assigning of 3s-, 3p- and 2p-XPS spectra of transition metals on the basis of the atomic multiplets theory are systematically laid out, for example, in [15]; they are outlined below.

The most simple are the 3s-spectra emitted in the process (1). The ground initial state term $^3F_4$ for the configuration $3d^8$ corresponding to a divalent nickel is well separated from other higher-energy terms, which makes it possible to consider all the atoms to be in the state $3d^8(^3F_4)$ prior to ionization. In the final state of photoionization, a high-spin state $3s^13d^8$ (^4F) and a low-spin state $3s^13d^8(^2F)$ are formed due to the interaction of the unfilled 3d-subshell with the 3s-vacancy with parallel and anti-parallel combination of their spins. It is those two states that are manifested in the 3s-spectrum if one neglects a small 3d-spin-orbit interaction, satellite processes, and the DPEO effect. Energy separation between the ^4F and ^2F components and their relative intensity are sensitive to the number of unpaired electrons on the transition metal ion, therefore these characteristics of the 3s-spectra can be used to determine the local spin and magnetic moment of [4, 6].

Qualitatively, the structure of the 3p-spectrum (process (2)) can also be described as a result of interaction between the spins of the 3p-vacancy and the $3d^N$-subshell: a 3p-specrum again can be roughly divided into the high-spin and the low-spin regions. Now, however, these are not single components but groups of component that have a rather complicated structure due to combined non-spherical electrostatic 3p-3d interaction and the spin-orbit interaction in the 3p-subshell. Additional important feature of the 3p-spectra is that the natural width of their components may vary within very broad limits, differing dozens of times for various $3p^5d^N(^{2S+1}L_J)$ components [19, 20]. This leads to difficulties in comparing theoretical and experimental spectra.

The main motive of the structure of the 2p-photoelectron spectra of 3d-metals (process (3)) is dictated by the spin-orbit splitting of 2p-subshell, and thus, in zero approximation, the 2p-spectrum is a spin-doublet $2p_{1/2,3/2}$. However, 2p-3d electrostatic interaction is sufficiently intense, and, as first shown by V.I. Nefedov [21], it leads to additional splitting of the components of the spin-doublet.

Results and discussion

The nickel complexes we have studied are mono−[Ni{$C_2(NH_2)_2(CN)_2$}$_2$] (I), Ni($C_{10}H_4(CH_3)_2N(SO_2C_6H_4(CH_3))$ (II), Ni(2,2'-bpy)$(OOCCMe_3)_2$ (III), $Ni_2(H_2O)$(2,2'-bpy)$_2(OOCCMe_3)_4$ (IV), Ni_2(2,4-Lut)$_2(OOCCMe_3)_4$ (V), where 2,4-Lut is 2,4-lutidine. The spatial structures of the complexes identified by the X-ray diffraction analysis [22, 23], are shown in Figure 1. Among the mononuclear complexes (I-III), the complex (I) has a planar square coordination of Ni, the complex (II) has tetrahedral, and the complex (III), distorted octahedral coordination. In the binuclear complexes (IV) and (V) the first coordination spheres around the Ni ions are also distorted octahedral, with one coordination site empty in (V).

Ni3s - x-ray photoelectron spectra of the complexes are shown in Figure 2, where they are compared with theoretical spectra calculated in this study (panels a, b), and in [17] (panel c). The heights of the vertical bars on the theoretical spectrum is proportional to the photoionization cross sections in process (1). When calculating the multiplet component energies, the exchange interaction integrals $G^2(3s3d)$ are scaled with a factor of 0.75. For comparison with experiment, each of the components of the theoretical spectrum in Fig. 2a, b, c is replaced with a Lorentzian profile with full width at half maximum (FWHM) of 5.5 eV. This value consists of the natural width of the 3s-level in the nickel atom and the broadening due to nonmonochromaticity of the $AlK\alpha_{12}$ excitation (1 eV). Calculated in configuration-average approximation [13] natural width of the Ni3s-level was 4.5 eV, which exceeds the results of the calculation [24] (2.89 eV), but close to the experimental value of the handbook [25] (4.4 eV). Our calculation (Fig. 2b) was carried out for the process (1) in the isolated-ion approximation The two main components of the theoretical spectrum correspond to the formation in the photoionization process (1) of the high-spin ($^4F_{9/2}$) and low-spin ($^2F_{7/2}$) states of in the final-state configuration $3s^13d^8$.

In the calculation [17] (Fig. 2c), in addition to the multiplet splitting, charge-transfer satellites were also taken into account, i.e., the photoionization processes into the states $3s^13d^9L^{-1}$, where L is ligand.

As seen from Fig. 2 (b, c), the calculated spectra are in satisfactory agreement with the spectra of the complexes (II-V), however, they differ sharply from the spectrum of complex (I) containing only one line.

As noted above, the environment of the nickel ion in the complex (II) is tetrahedral, while in the complexes (III-V) it is distorted octahedral. With regard to the influence of crystal field, the electronic configurations of the $3d^8$-subshell can be written as follows: $e_g^4t_{2g}^4$ (tetrahedron) and $t_{2g}^6e_g^2$ (octahedron). It is obvious that in both cases there are two unpaired electrons. Thus, Ni3s-spectra of the complexes (II-V) should be similar to each other and to the spectrum of the $3d^8$ ion, which is indeed the case, see Fig. 2.

For the complex (I) with a planar square coordination, the configuration of 3d-electrons is $e_g^4a_{1g}^2b_{2g}^2b_{1g}^0$. An alternative high-spin configuration $e_g^4a_{1g}^2b_{2g}^1b_{1g}^1$ is not realized because of the substantial energy separation of the b_{1g} level. Thus, the 3d-electrons in (I) are all in completely filled levels. This corresponds to zero total spin of the nickel ions and diamagnetic nature of (I). After 3s-ionization on the background of completely filled levels, there appears only a single state $3s^1$, which gives one line in the 3s-photoelectron spectrum. In the isolated-ion approximation, the situation in the complex (I) can be simulated with the atomic configuration $3d^{10}$. The result of such a calculation is shown in Figure 2a. The experimental spectrum of (I) confirms the above considerations. Our data thus

demonstrate the sensitivity of X-ray photoelectron spectra of the 3d-elements in compounds to the geometry of the nearest environment, and support the data of X-ray diffraction studies [22, 23].

Experimental Ni3p-spectra of the compounds are shown in Figure 3, where they are compared with calculated spectra for atoms in configurations $3d^{10}$ (panel a) and $3d^8$ (panel b). In the calculation of the 3p-spectra the integrals of electrostatic interactions were scaled with the factor 0.77. As mentioned above, the 3p-spectra of transition metals with unfilled 3d-subshells have an important feature - the natural widths of their components may differ very much. The reason for this is a strong dependence on the term of the partial widths associated with a very rapid 3p-3d3d Coster-Kronig transition from the photoionization final states, $3p^5 3d^N(^{2S+1}L_J)$. The same phenomenon is seen in the 4p-spectra of 4d-transition elements and in the 4d-spectra of 4f-transition elements (see [13] and references therein).

Rigorous calculation of widths of each component of the XPS is a very complicated problem and up to now there exist only a few works where calculations are performed straightforwardly. In particular, such calculations were carried out for the 3p-XPS of atomic nickel in [20], where the experimental spectrum of atomic nickel was also obtained. It follows from the results of [20] that the natural widths of the Ni3p-spectrum components increase from several tenths of electron volts to about 6 eV with the growth of the binding energy. Our calculation of the average width of the $3p^{-1}3d^8$ states gave a value of 2.9 eV. Based on the results of [20], the width of the components of the theoretical spectrum in Fig. 3 were selected as follows. The spectrum was divided into three regions of the binding energy: from 67 to 69.5 eV, from 69.9 to 76 eV and from 75 to 84 eV. The widths of the components in those areas were taken equal to 0.2 eV, 3 eV and 6 eV, respectively. In order to account nonmonochromaticity of excitation, the spectrum thus obtained was further convoluted with a Lorentzian function with FWHM= 1 eV. The spectrum calculated in this way is shown in Fig. 3b, it is in good agreement with the atomic experiment and the calculation of [20].

Based on the considerations on the splitting of the 3d- levels by the crystal field outlined above, it is expected that the spectrum calculated in the ionic configuration $3d^8$ (process (2)), should be similar to the spectra of high-spin complexes. (II-V), which is indeed observed, see Fig. 3. At the same time, for the diamagnetic complex (I) the spectrum should be similar to that of the nickel atom with a completely filled 3d-shell, and be a spin-doublet $3p_{1/2,3/2}$. Fig. 3a shows the spectrum calculated in this approximation, which, as can be seen, fits well the spectrum of complex (I).

Measured and calculated Ni2p-spectra are shown in Fig. 4. The calculations were performed for the configuration $3d^{10}$ simulating the diamagnetic complex (I), and the configuration $3d^8$ simulating the complexes (II-V). In calculating the profiles of the spectra we used in the experimental natural widths of the L_2- and L_3-levels, 2 eV and 1.6 eV, respectively [25]. The spectra were additionally broadened with the Lorentzian with FWHM of 1 eV to account for nonmonochromaticity of excitation.

In the case of a closed 3d-subshell (Fig. 4a) theoretical Ni2p-spectrum represents the pure spin-doublet and agrees well with the experimental spectrum of the diamagnetic complex (I).

The calculation for the process (3) modeling the photoabsorption in the complexes with two unpaired 3d-electrons (Fig. 4b) reproduces only the main components of the spectra. The experimental spectra of complexes (II-VI) contain intense satellite structures at the binding energies of 862 eV and 881 eV. These structures are associated with the charge-transfer satellites; they cannot be reproduced in the isolated-ion approximation used in this study. It should be noted that similar features are also seen in the spectrum of complex (I), but there, they are much less intense and much more shifted from the main peaks.

Note that the charge-transfer satellites are also present in Ni3s-and Ni3p-spectra, but there they are superimposed on the components of the spectra associated with the multiplet splitting and do not appear as separate components. Exceptions are the spectra of complex (I), where the multiplet splitting is absent. The 3s-and 3p-spectra of this compound (see Fig. 2, 3) contain weak intensity broad components, essentially shifted from the main peaks, which apparently can also be attributed to the charge-transfer satellites.

The absence of intense satellites in the spectra of the nickel complexes with a planar square coordination was noted by other authors [26]. The authors of [26] even proposed to use this feature to identify the square complexes. Significant difference in the behavior of the charge-transfer satellites in Ni2p-spectra of the diamagnetic and paramagnetic complexes can be explained by the different character of the splitting of 3d-shell crystal field in these complexes.

In the framework of the charge-transfer satellite theory [15] one should take into account the mixing of the ground state $3d^N\mathrm{L}$ and charge-transfer states $3d^{N+k}\mathrm{L}^{-k}$ (L=ligand) in initial and final states of photoabsorption. The intensity of the charge-transfer satellites is determined by the degree of admixture of the $3d^{N+k}\mathrm{L}^{-k}$ state to the ground state. The latter parameter is significantly affected by the so-called charge-transfer energy (the Δ parameter), which, in zero approximation, can be taken equal to the energy separation of the satellites from the main line.

In the first order perturbation theory the square of the participation coefficient of the excited state decreases with increasing Δ as Δ^{-2}. The intensity of the charge-transfer satellites must obey approximately the same law. It is seen from Figure 4 that upon going from the high-spin complexes (II-V) to the diamagnetic complex (I), the energy separation of satellites increases approximately 1.6 times. Then one should expect that in the complex (I) the intensity of the satellites will be approximately 2.6 times less. Roughly, this satellite intensity decrease is indeed observed in the experiment.

The reason for significant differences between the charge-transfer energy in the high- and low-spin complex is following. In a tetrahedral complex (II) and octahedral complexes (III-V) excitation

L→3*d* is possible directly to the highest partially filled orbitals, t_{2g} and e_g, respectively. In the case of a flat square complex (I) for this excitation it is necessary to spend additional energy equal to the energy difference between the vacant orbital b_{1g} and the highest fully occupied orbital b_{2g}.

Note that our experimental data allow determining the energy splitting between the b_{2g} and b_{1g} orbitals of the quadratic complex (I). It is equal to the difference between the energy separations of the charge-transfer satellites in the plane quadratic and octahedral complexes and is, as seen from Fig. 4, 2.5 ± 0.3 eV.

Table. 1 lists the energies of the main lines of Ni3s, Ni3p and Ni2p-spectra. Figure 5 shows the energy shifts of the main lines of Ni3s, Ni3p and Ni2p spectra relatively to the lines positions in the complex (I) Analysis of changes in the positions of the lines of the photoelectron spectra of nickel makes it possible to study the variation of electron density on the metal ion in the complexes when going from one compound to another.

It is seen from Table 1 and Figure 5 that upon going from one compound to the other, similar (within the experimental error) changes take place in all the spectral lines of Ni. We note that the contrast of these changes is greater for the deeper initial vacancies created in the photoionization process. This is consistent with the qualitative idea of the localization of vacancies - the deeper the vacancy is, the more is the state is localized, and therefore, the more sensitive it is to the local charge on the atom.

It is evident from Figure 5 that upon going from complex (I) to complex (II) there is a significant increase in binding of the main spectral lines. The increase in the binding energies of photoelectron lines indicates a decrease in electron density on the nickel ion when going from (I) to (II). This decrease is explained by a radical change in the geometry of the nearest environment of the metal atom. Indeed, the complex (I) has a planar coordination (see Fig. 1). In this case there is a significant transfer of electron density from ligands to the metal atom via the π-system, and the binding energy of the photoelectron lines are small. In the complex (II) with a tetrahedral geometry of the nearest environment π-system is absent, transfer of the electron density decreases, the local ionic charge and the binding energies of the lines of the photoelectron spectra increase.

Upon going from (II) to (III), tetrahedral environment is replaced by octahedral, the number of the nearest-neighbor ligand atoms around Ni atoms increases from four to six, electron density transfer increases; this reduces the local charge on the nickel atom and the lines' binding energies.

In complexes (III) and (IV) environment is distorted octahedral, and, despite the fact that the sets of nearest-neighbor atoms are not identical, the local charge on the nickel atom is changed, apparently, insignificantly. This is reflected in the fact that the positions of the XPS lines in these complexes remain unchanged within the experimental accuracy.

For the complex (V), the increase of the binding energies is seen, which is evidence of the decrease in electron density on the nickel atoms. This decrease is associated with the decrease of the number of nearest-neighbor atoms around Ni down to five in (V) (see Fig. 1).

The above data confirm the results of the X-ray diffraction studies [22, 23].

Conclusion

Electronic and spatial structure of mono-and binuclear carboxylate complexes of nickel was studied by X-ray photoelectron Ni3s, Ni3p iNi2p spectra. Assignment of the spectra is performed on the basis of calculations in the isolated-ion approximation. The dependence of spectral profiles, line positions, and charge-transfer satellites structures on the structure of nearest-neighbor environment of nickel (II) in complexes is discovered. Our results demonstrate the potential of XPS as a tool for studying electron and spatial structure of metalloorganic complexes.

Acknowledgements

This work was supported by the Russian Foundation for Basic Research (project 09-03-00157), the Council on Grants of the President of the Russian Federation (Program for Support of Leading Scientific Schools - Grant NSH-3672.2010.3), the Ministry of Education and Science (SC-14.740 .11.0363), the Presidium of Russian Academy of Sciences.

References

[1] V.V. Pavlishchuk, Teoreticheskaya i Eksperimentalnaya Khimiya (Russia) 33(1997) N6. 341.

[2] I.L.Eremenko, S.E. Nefedov, A.A. Sidorov,M.A. Golubnichaya, P.V. Danilov, V.N. Ikorskiiu, Yu.G. Shvedenkov, V.M. Novotortsev, I.I. Moiseev I, Inorg. Chem. 38(1999) 3764.

[3] D.W. Boukhvalov, M.Al-Saqer, E.Z. Kurmaev, A. Moewes, V.R. Galakhov, L.D. Finkelstein, S. Chiuzbăian, M. Neumann, V.V. Dobrovitski, M.I. Katsnelson, A.I. Lichtenstein, B.N. Harmon, K. Endo, J.M. North, N.S. Dalal, Phys. Rev. B. 75(2007) 014419.

[4] A.G. Kochur, T.M. Ivanova, A.V. Shchukarev, R.V. Linko, A.A. Sidorov, M.A. Kiskin, V.M. Novotortsev, I.L. Eremenko. J. Electron Spectrosc. Relat. Phenom 180 (2010) 21.

[5] M.A. Kiskin. Magnrtoactive polymere pivalates of Mn (II) anf Fe(II): synthesis, structure, magnetic properties, and chemical activity. Thesis Cand. Chem. Sci. Kurnakov Institute of General and Inogranic Chemistry of RAS, Moscow, 2005.

[6] A.G. Kochur, T.M. Ivanova, A.V.Shchukarev, A.A. Sidorov, M.A. Kiskin, V.M. Novotortsev, I.L. Eremenko. Bulletin of the Russian Academy of Sciences: Physics. 74 (2010) No.5. 625.

[7] T.M. Ivanova, A.V. Naumkin, A.V. Shchukarev, A.A. Sidorov, M.A. Kiskin, V.M. Novotortsev, I.L. Eremenko. Bulletin of the Russian Academy of Sciences: Physics. 72 (2008) No. 4. 519.

[8] T.M.Ivanova, A.G.Kochur , A.V.Shchukarev A.A.Sidorov, M.A.Kiskin, V.M.Novotortsev, I.L.Eremenko. Russian Journal of Inorganic Chemistry. 54 (2009) No. 10. 1637.

[9] T.M. Ivanova, A.V. Naumkin, A.A. Sidorov, M.A. Kiskin, I.L. Eremenko J. Electron Spectrosc. Relat. Phenom. 156-58 (2007) 200.

[10] A.G. Kochur, T.M. Ivanova, A.V. Shchukarev, R.V. Linko, N.G. Terebova, A.A. Sidorov, I.L. Eremenko. Russian Journal of Inorganic Chemistry. 56 (2011) No. 3. 402.

[11] T.M. Ivanova, A.V. Naumkin, A.A. Sidorov, M.A. Kiskin, V.M. Novotortsev, I.L. Eremenko. Zurnal Neorganicheskoi Khimii.52 (2007) №11. 1892.

[12] Ferrgina C.J., Massucci M. // Inclussion Phenomena and Molecular Recognition in Chemistry. 1989. N7. 529.

[13] A.G. Kochur, I.D. Petrov, J. Schulz, Ph. Wernet. J. Phys. B: At. Mol. Opt. Phys. 41 (2008) 215002.

[14] R. Kau, I.D. Petrov, V.L Sukhorukov, H. Hotop. Z. Phys. D **39** (1992) 262.

[15] F. de Groot. Multiplet effects in X-ray spectroscopy. Coordination Chemistry Reviews 249 (2005) 31.

[16] V.F. Demekhin, V.L. Sukhorukov, V.A. Yavna et al. Izv. Acad. Nauk USSR. Ser. Fiz. 40 (1976) No 2. 255.

[17] E. Stavitski, F.M.F. de Groot. Micro. 41 (2010) 687.

[18] V.L.Sukhorukov, I.D.Petrov, V.F. Demekhin, S.V.Lavrentiev. Izvestiya Akademii Nauk USSR. Ser. Fiz. 49 (1985) № 8. 1463.

[19] M. Taguchi, T.Lozumi, A.Kotani. J. Phys. Soc. Japan. 66 (1997) No 1, 247.

[20] K. Tiedtke, Ch. Gerth, B. Kanngießer, B. Obst, P. Zimmermann, M. Martins and A. Tutay. Phys. Rev. A. 60 (1999) 3008.

[21] V.I.Nefedov Bull. Acad. Sci.USSR. Ser.Phys. 28 (1964) 728 (translated from Nefedov V.I. Dokl. Akad. Nauk. Ser.Phys. 28 (1964) 816.

[22] I.L.Eremenko, V.M. Novotortsev, A.A. Sidorov, I.G. Fomina. Russia Chem. J. XLVIII (2004) 49.

[23] I.L.Eremenko, S.E. Nefedov, A.A. Sidorov, M.A. Golubnichaya, I.F. Golovaneva, V.I. Byrkov, O.G. Ellert, V.M. Novotortsev, L.T. Eremenko, A. Soysa, M.R. Berezhko. Izvestiya Akademii Nayk, Ser. Chem. (1998). N4. 725.

[24] M.O.Krause, J.H.Oliver. J. Phys. Chem. Ref.Data. 8 (1979) No 2. 329.

[25] M.A.Blokhin, I.G.Shveitser. X-ray Spectroscopy Reference book .Moscow: Nauka. 1982.

[26] L.J.Matienzo, W.E.Swartz, Jr, S.O.Grim. Inorg. Nucl. Chem. Lett. 8 (1972) 1085.

Table 1.

Peak energy of the main lines of X-ray photoelectron spectra (in eV)*

Compound	Ni3*s*	Ni3*p*	Ni2$p_{3/2}$
(I)	112.8	68.3	855.2
(II)	113.8	68.9	856.4
(III)	113.0	68.2	855.7
(IV)	112.9	68.3	855.7
(V)	113.3	68.6	856.0

*absolute error of measurement is 0.1 eV

Figures captions

Fig.1.

Spatial structures of complexes mono−[Ni{$C_2(NH_2)_2(CN)_2$}$_2$] (I), Ni($C_{10}H_4(CH_3)_2N(SO_2C_6H_4(CH_3)$ (II), Nibpy($OOCCMe_3$)$_2$ (III), $Ni_2(H_2O)bpy_2(OOCCMe_3)_4$ (IV), Ni_2(2,4-Lut)$_2$($OOCCMe_3$)$_4$ (2,4-Lut=2,4-lutidine) (V). R=$C(CH_3)_3$

Fig. 2.

Experimental Ni3s-spectra of the complexes (I – V) and Ni3s-spectra of the Ni atoms in configurations $3d^{10}$ and $3d^8$, calculated in this study (a, b). The calculation of [18] is in panel (c). To compare with experiment, the theoretical components of the spectra were changed with the Lorentzian profiles with the FWHM of 5.5 eV

Fig. 3.

Experimental Ni3p-spectra of the complexes (I – V) and calculated Ni3p-spectra of the Ni atoms in configurations $3d^{10}$ and $3d^8$ (a, b). For comparison with the experiment, the component of the theoretical spectrum are replaced by Lorentzian profiles of different widths (see text) and further broadened by the Lorentzian distortion with FWHM of 1 eV.

Fig. 4.

Experimental Ni2p-spectra of the complexes (I – V) and calculated Ni2p-spectra of the Ni atoms in configurations $3d^{10}$ and $3d^8$ (a, b). For comparison with the experiment, the component of the theoretical spectrum are replaced by the Lorentzian profiles with FWHM of 2.6 eV ($2p_{3/2}$) and 3.0 eV ($2p_{1/2}$).

Fig . 5.

Shifts of the main lines peaks in the photoelectron spectra of nickel compounds (I-V)

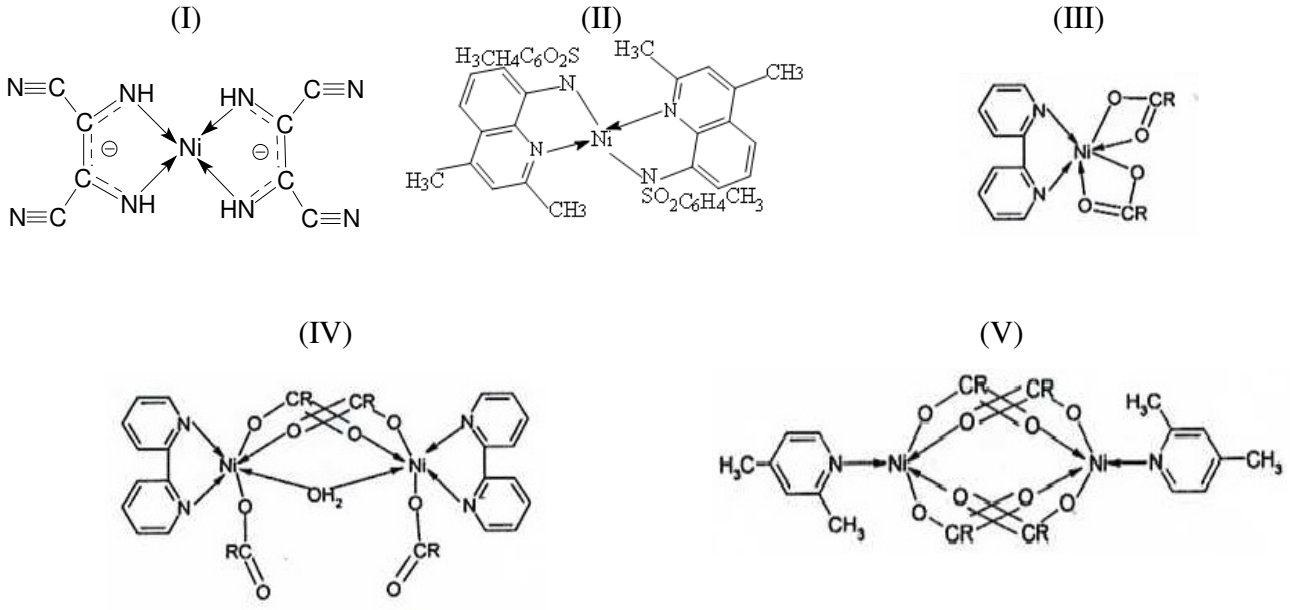

Fig.1 Kochur

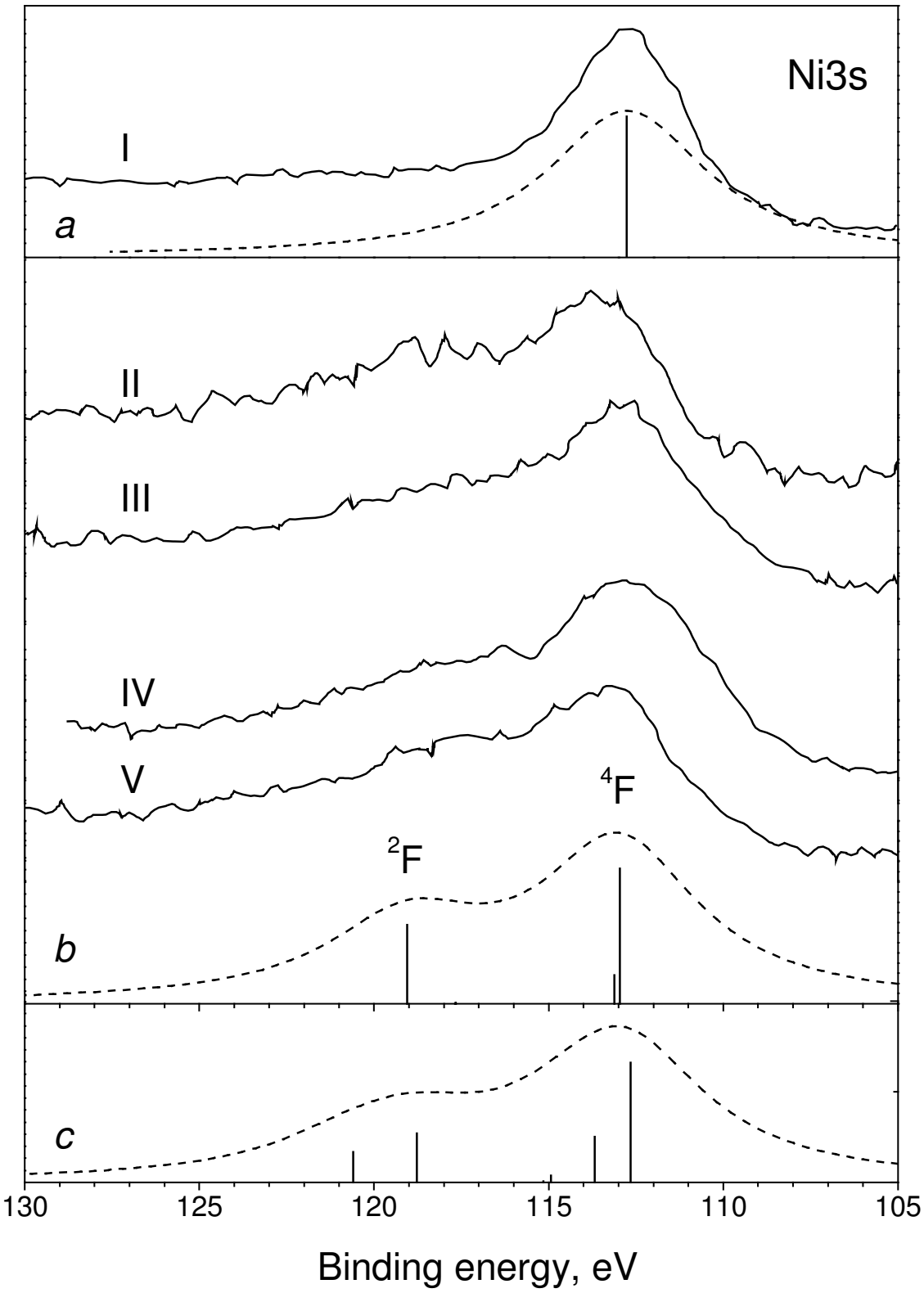
Ni3s
I
a
II
III
IV
V
^{4}F
^{2}F
b
c
130
125
120
115
110
105
Binding energy, eV

Fig.2 Kochur

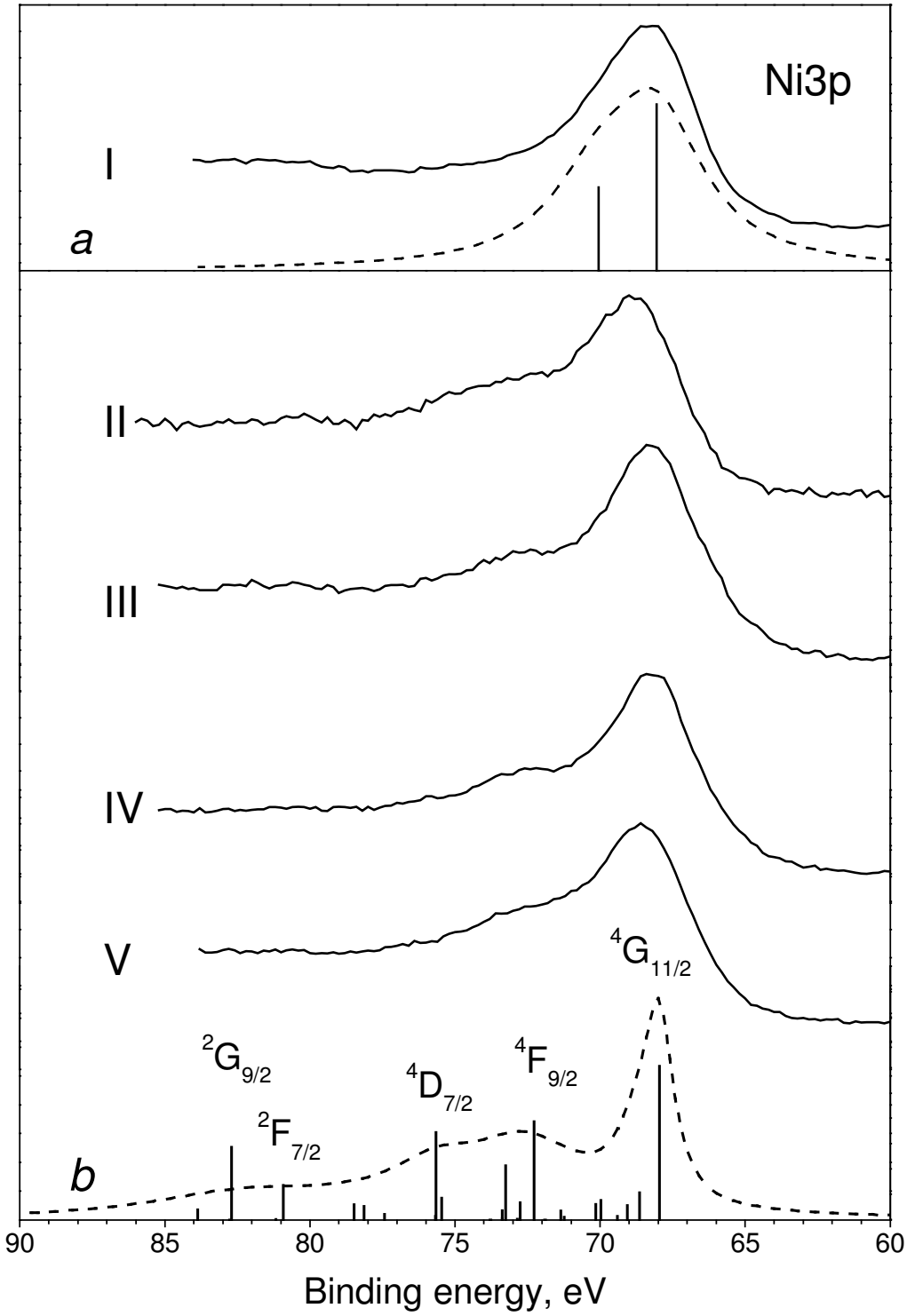
Ni3p
I
a
II
III
IV
V
$^4G_{11/2}$
$^2G_{9/2}$
$^4D_{7/2}$
$^4F_{9/2}$
$^2F_{7/2}$
b
90
85
80
75
70
65
60
Binding energy, eV

Fig.3 Kochur

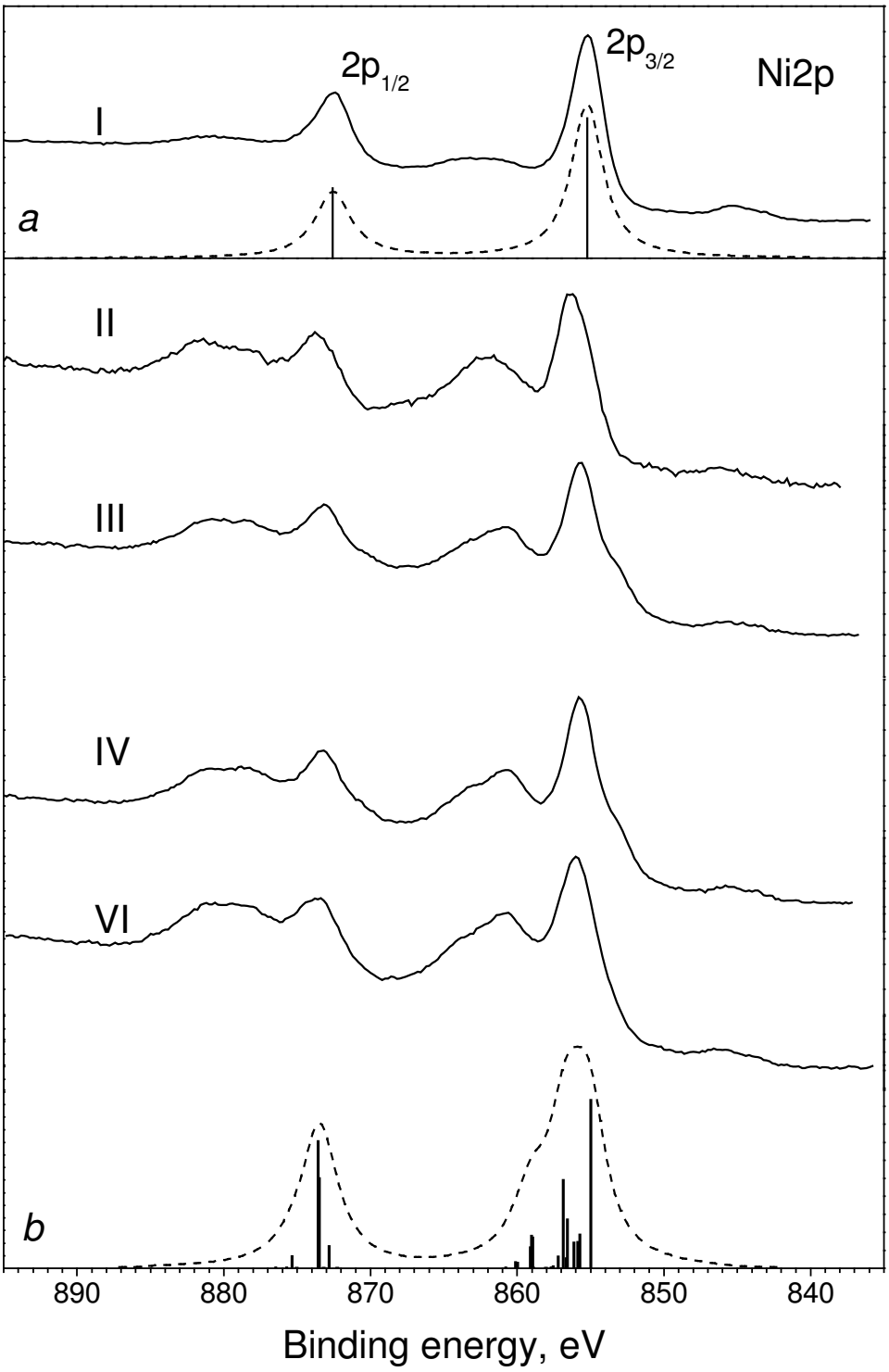
2p1/2
2p3/2
Ni2p
I
a
II
III
IV
VI
b
890
880
870
860
850
840
Binding energy, eV

Fig.4 Kochur

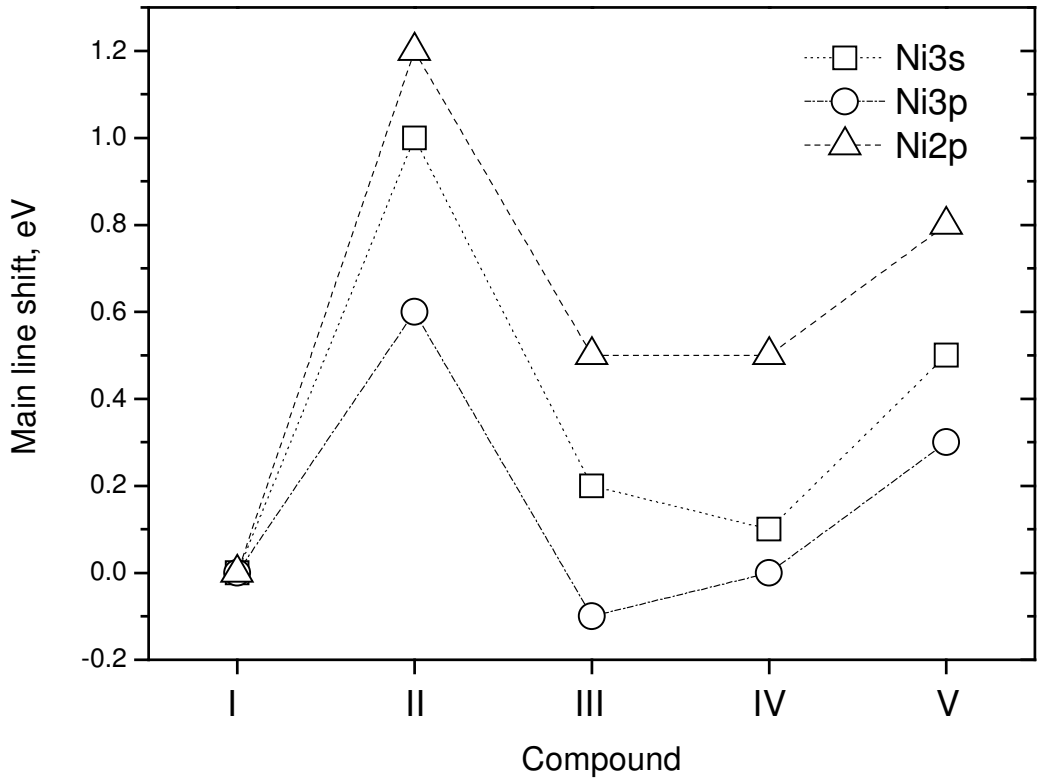
Ni3s
Ni3p
Ni2p
Main line shift, eV
1.2
1.0
0.8
0.6
0.4
0.2
0.0
-0.2
I
II
III
IV
V
Compound

Fig.5 Kochur